

Electrical properties of $\text{SrBi}_2\text{Ta}_2\text{O}_9$ single crystals grown by self-flux solution

H. Amorín, M.E.V. Costa*, A. L. Kholkin, J. L. Baptista

Department of Ceramic & Glass Engineering, CICECO, University of Aveiro, Aveiro 3810-193, Portugal

Abstract

High-quality $\text{SrBi}_2\text{Ta}_2\text{O}_9$ single crystals were grown by a self-flux solution method using Bi_2O_3 added with B_2O_3 flux. Chemical composition corresponded to the formula $\text{Sr}_x\text{Bi}_y\text{Ta}_2\text{O}_9$ where $x = 1.03 \pm 0.05$ and $y = 1.87 \pm 0.08$. Transparent SBT crystals obtained by slow cooling (2°C/h) of the melt from 1350°C to 1100°C , exhibit platelet morphology with typical sizes of $5 \times 3 \times 0.05 \text{ mm}^3$ dimensions with a dominant (001) orientation of a major face. Ferroelectric hysteresis and dielectric properties are measured perpendicularly to the major face of the crystals. Anisotropy, crystalline orientation, growth mechanism, and their influence on electrical properties are discussed.

© 2003 Elsevier Ltd. All rights reserved.

Keywords: Bi-layered ferroelectrics; Ferroelectric properties; Self-flux growth; $\text{SrBi}_2\text{Ta}_2\text{O}_9$ single-crystals

1. Introduction

Along with the $\text{Pb}(\text{Zr}_x\text{Ti}_{1-x})\text{O}_3$ (PZT) system, Bi layer-structured ferroelectrics, in particular $\text{SrBi}_2\text{Ta}_2\text{O}_9$ (SBT), have attracted much attention as new promising candidates for nonvolatile Ferroelectric Random Access Memories (FeRAMs). Contrary to PZT, SBT demonstrates a relatively high fatigue endurance and low leakage of current density.^{1–3} SBT is a member of the Aurivillius family having a layered structure⁴ where pseudoperovskite blocks $(\text{SrTa}_2\text{O}_7)^{2-}$ are interleaved with $(\text{Bi}_2\text{O}_7)^{2+}$ layers.⁵

A large amount of work has been undertaken on SBT ceramics and thin films.^{6–9} Ferroelectric properties were found to depend strongly on their complex micro- and defect structure and on crystallographic orientation. It is becoming very important to control processing and texturing conditions to overcome difficulties in investigating the intrinsic properties of SBT materials. To accelerate piezoelectric transducer development, it is important to understand the single crystal (intrinsic) properties of the ferroelectric SBT system. Perfect single crystals have to be grown and studied in their single domain state or at least under controlled domain conditions. However, there are only a few reports on SBT

single crystals,^{10,11} where the maximum crystal growth reported so far is in the range 0.3–1 mm and was too small for further studies. Recently, large high-quality SBT single crystals were synthesized for the first time, using a modified self-flux solution.¹²

In this paper, the processing of large SBT single crystals grown via a high-temperature self-flux solution method is reported. Structural and electrical properties are discussed in terms of the anisotropy, crystalline orientation and growth mechanism of the SBT crystals.

2. Experimental procedure

SBT single crystals were grown using a high-temperature modified self-flux solution method described elsewhere.^{11–14} Polycrystalline SBT powder was first synthesized via a solid-state reaction using high-purity ($\geq 99.9\%$) SrCO_3 , Bi_2O_3 and Ta_2O_5 reagents. The compounds were mixed in stoichiometric amounts in ethanol until the mixture appeared homogenous. The mixture was put in a 15 ml volume platinum (Pt) crucible sealed with a Pt lid, and then placed in a large sealed alumina crucible to minimize Bi evaporation. Pure SBT powder was obtained by heating to 950°C at a rate of 300°C/h , soaking in air at this temperature for 2 h, and then cooling to room temperature.

After the firing process, the SBT powder was vigorously ground by ball milling in ethanol for 12 h, using

* Corresponding author. Tel.: +351-24-370354; fax: +351-24-25300.

E-mail address: elisabete@cv.ua.pt (M.E.V. Costa).

zirconia balls in a polyethylene jar. After milling, the powder was mixed with the flux, using a SBT/flux ratio of 50/50 until a homogenous mixture was reached and dried at 120 °C. Bi₂O₃ (melting point of 825 °C) and a small amount of B₂O₃ (melting point of 450 °C) were used as a flux, because B₂O₃ considerably lowers the melting point of the SBT phase and results in a more stable flux with crystals nucleating in a highly viscous medium.¹² Well-ground mixture (40 g) was put in the 15 ml volume Pt crucible and was sealed with the Pt lid. The alumina crucible was also sealed to minimize Bi evaporation. Then, a premelting was done at 950 °C for 2 h. The temperature profile for crystal growth includes heating to 1350 °C, soaking at this temperature for 10 h, and a slow cooling at 2 °C/h down to 1100 °C.¹²

The grown SBT crystals were separated from the flux using a two-step process. A porous ceramic was used at

1000 °C to separate the flux from Pt and then leached in 30% hot HNO₃ to dissolve the flux and to separate the crystals. This process was slow and took a few days to complete removing the flux between single crystal platelets.

The structure of single crystals was examined by X-ray diffraction analysis (XRD) using a Rigaku/New diffractometer (CuK_α radiation, 0.05°/step). The reflections obtained were analyzed by means of the Jade6 XRD pattern processing and the 2000 PDF database. This allowed us to identify the crystalline phase present in the crystals. The transverse section of the crystal was examined using a Zeiss optical microscope with a JVC camera connected to a PC. Ferroelectric hysteresis was measured using a TF Analyzer (AIXACT) at room temperature. Dielectric properties were measured using a HP4284A precision LCR Meter in the frequency range from 1 kHz–1 MHz with the temperature controlled by an Eurotherm 2404 controller. Single crystal platelets of about 5×3×0.05 mm³ were polished using diamond paste for electrical characterization. Gold layers were sputtered onto the parallel polished facets. The chemical composition of the single crystals was analyzed using a Jobin Yvon (Jy70 Plus) Inductively Coupled Plasma-Optical Emission Spectroscopy (ICP) and determined to be Sr_xBi_yTa₂O₉ where $x = 1.03 \pm 0.05$ and $y = 1.87 \pm 0.08$.

3. Results and discussion

3.1. Single crystal growth

High-quality SBT single crystals could be obtained only by using a low B₂O₃ content in the Bi₂O₃ based flux. It was found that without B₂O₃ inclusion the SBT powder does not melt thoroughly at 1350 °C (5 h dwell time), due to the high melting point of the SBT phase, resulting in a dense ceramic into the solidified flux. The mole ratio of the SBT composition to flux (SBT/Flux) was 50/50 in this case. Small crystals were formed around the platinum lid in the vapor phase region.¹⁵ These crystals were powdered and attributed to the SBT phase by XRD. A small amount of a tetragonal phase isostructural to SrTa₄O₁₁ was also observed [see Fig. 1(a)]. Crystals were very small (≤0.5 mm) and it was very difficult to separate them for electrical characterization. Therefore, they were not studied.

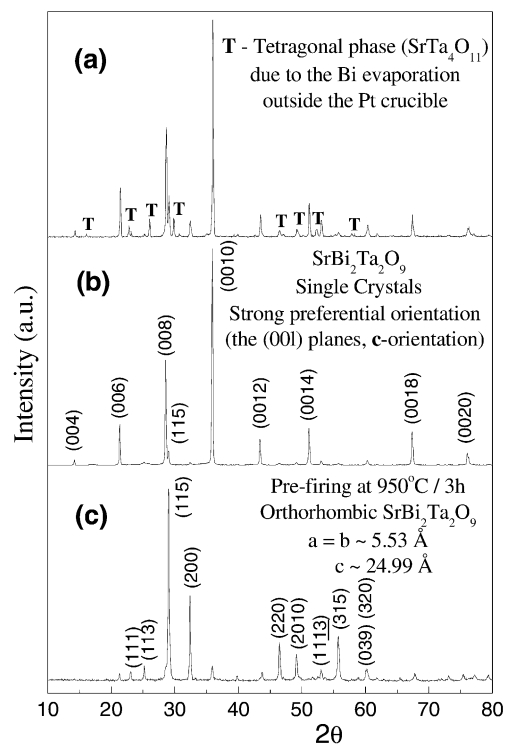


Fig. 1. XRD patterns for: (a) SBT single crystals formed around the platinum lid in the vapor phase region using Bi₂O₃-based flux without B₂O₃ inclusion, together with a tetragonal phase isostructural to SrTa₄O₁₁; (b) c-axis oriented SBT single crystal platelet containing small amount of non-(00l) oriented areas; and (c) pure orthorhombic SBT powder pre-fired at 950 °C over 3 h.

Table 1
Results of crystal growth with different flux compositions

Concentration (wt%)		Grown Crystals	Maximum size (mm)	Color	Habitus
Bi ₂ O ₃	B ₂ O ₃				
50	0	SBT + SrTa ₄ O ₁₁	≤1×1	—	—
45	5	SBT	5×3	Translucent	Layers

A small concentration of B_2O_3 (mole ratio of $\text{B}_2\text{O}_3/\text{Bi}_2\text{O}_3$ equal to 5/45) considerably lowers the melting point of the SBT phase and results in a more stable flux, with crystals nucleating in a highly viscous medium.¹² These results are summarized in Table 1.

Very translucent high-quality single crystal platelets were obtained with a boron-modified flux, as shown in Fig. 2(a). Crystal size was about $5 \times 3 \text{ mm}^2$ with thickness varied from 50 to 100 μm . Fig. 1(b) shows the XRD pattern of a typical SBT single crystal plate where (00l) reflections are much stronger than the (hk0) reflections [see XRD of a pure as-fired SBT polycrystalline powder in Fig. 1(c)]. Highly oriented SBT single crystal platelets (with the c -axis perpendicular to the major face) are obtained. This result suggests the higher growth rate of this system in the a - b plane, as compared to that in the c -axis direction.

From the point of view of the SBT structure [an orthorhombic distorted structure with space group $A2_1am$, in which pseudoperovskite blocks (SrTa_2O_7)²⁻ interleave with (Bi_2O_7)²⁺ layers]¹⁶ growing in a homogeneous flux medium, the easy growth of the single crystal in the a, b -axis directions is well understood, since all the ions needed are available at the same time [see Fig. 2(b) for better understanding]. In the c -axis, this growth is much more complex because both, the

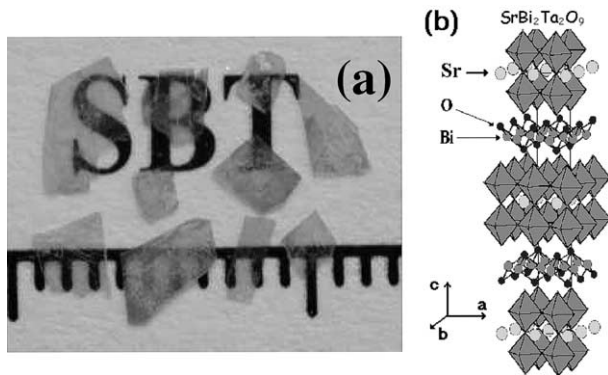


Fig. 2. (a) Top view of transparent $\text{SrBi}_2\text{Ta}_2\text{O}_9$ single crystals platelets washed in 30% HNO_3 hot acid for several days (1 division = 1 mm). (b) Lattice structure of $\text{SrBi}_2\text{Ta}_2\text{O}_9$ system (pseudoperovskite (SrTa_2O_7)²⁻ blocks interleaved with (Bi_2O_7)²⁺ layers).^{16–18}

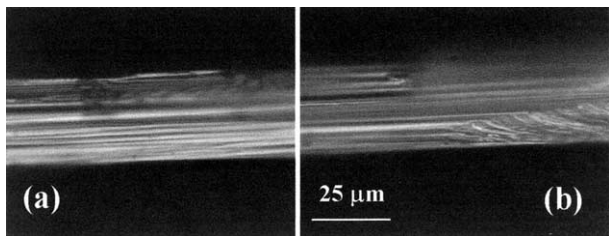


Fig. 3. Transverse section of the SBT single crystal by optical microscopy, where several layers are lying at an angle relative to the crystal major face interface with layers stuck parallel to the major face in some regions. These layers are possibly associated with oriented thinner crystals parallel to the a - b planes.

pseudoperovskite (SrTa_2O_7)²⁻ blocks and the (Bi_2O_7)²⁺ layers, should not be delivered at the same time. That is why, in general the crystals were inhibited from growing freely in three dimensions and new crystals always nucleate over the surface of another single crystal. Instead of having fewer single crystals of a large size, multiple nucleations occur leading to many small-sized platelets.

It should be noted, however, that small reflections of non-(00l) peaks were obtained in the XRD patterns. Therefore, some platelets may contain small volumes with orientations other than (00l), which are probably due to twinning during crystal growth. Fig. 3 shows the transverse section of a crystal by optical microscopy. As can be seen in Fig. 3(a), several layers oriented parallel to the major face can be distinguished in cross-sections. These layers are possibly associated with several thinner crystals stuck parallel to the a - b plane. However, Fig. 3(b) shows layers that are lying at some angle relative to the plane of the crystal face, interfacing with the parallel layers. This can be related to the twinning

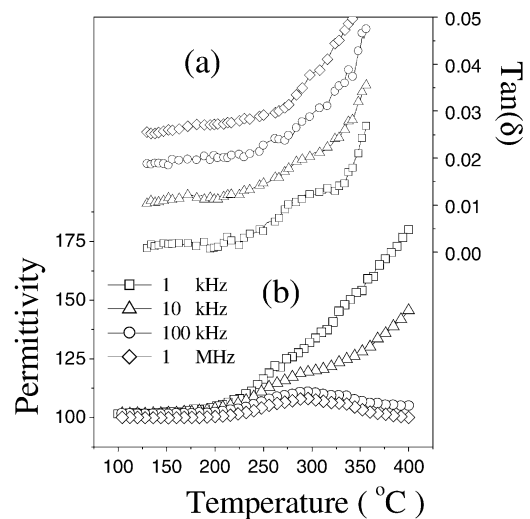


Fig. 4. Temperature dependence of: (a) dielectric losses; and (b) permittivity at several frequencies measured perpendicularly to the major face of the crystal.

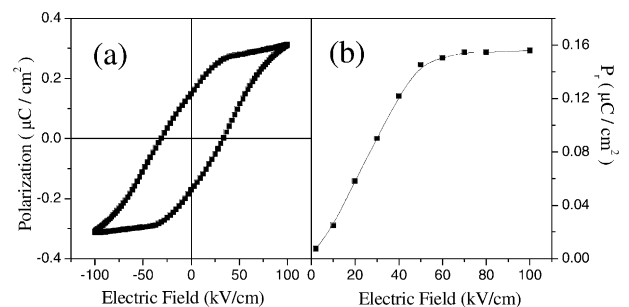


Fig. 5. (a) Saturated ferroelectric hysteresis loop for a maximum electric field of 100 kV/cm (b) Remanent polarization vs maximum electric field at room temperature in the SBT crystal.

defects and may be a reason for XRD results showing some reflections other than (00l).

3.2. Ferroelectric properties

Dielectric losses and permittivity of the SBT crystals were measured at different frequencies under cooling and are depicted in Fig. 4. A maximum was obtained around 300 °C, which can be associated with the ferroelectric phase transition. Low permittivity values were recorded in the entire temperature range ($\epsilon' \approx 120$ in the maximum) and were significantly smaller than the values for SBT ceramics ($\epsilon'_{\max} \approx 600$), while low dielectric loss was recorded in the entire ferroelectric region ($\tan\delta \leq 0.03$). This can be attributed to the almost perfect *c*-axis orientation of the single crystal. Ceramics contain all possible orientations of crystallites, including highly polarizable *a*–*b* planes, therefore, both permittivity and loss factor are higher than in the investigated crystals.

Hysteresis measurements were made to confirm the ferroelectric behavior below the phase transition on 50 μm thick single crystals. Fig. 5 shows saturated hysteresis loop obtained in this crystal with a very low remanent polarization ($P_r < 0.2 \mu\text{C}/\text{cm}^2$), consistent with dielectric measurements. The maximum electric field applied was 100 kV/cm, higher than that reported for SBT single crystals.^{11,12} This demonstrates the high quality of our crystals, where low leakage and a high breakdown field can be achieved, through a bismuth layer structure along the *c*-axis direction.^{1–3}

The polarization vector in the SBT orthorhombic structure lies entirely along the *a*-axis, having a miller plane along *c*-axis.^{17,18} Polarization experimentally observed in the direction normal to major face in our samples should be associated with the contribution of the non-(00l) oriented crystallites, i.e. due to the contribution from *a*–*b* planes that are not parallel to the major face of the sample, as confirmed by XRD and optical microscopy. Further investigation is underway to clarify the correlation between the experimentally observed polarization and volume ratio of non-*c*-axis oriented crystallites. Atomic Force Microscopy in a piezoelectric mode will be applied in order to reveal both in-plane and out-of-plane components of polarization.

4. Conclusions

High-quality SBT single crystals were obtained using a low content of B_2O_3 in the Bi_2O_3 based flux using a high-temperature self-flux solution method. The chemical composition was determined by electron probe microanalysis and corresponded to the formula $\text{Sr}_x\text{Bi}_y\text{Ta}_2\text{O}_9$ where $x = 1.03 \pm 0.05$ and $y = 1.87 \pm 0.08$.

Transparent SBT single crystals exhibited a dominant (00l)-orientation with small reflections of non-(00l) peaks, appearing probably from twinning defects. Layered habitus was obtained with relatively large single-crystal surface areas: $5 \times 3 \text{ mm}^2$ and only 50 μm in thickness. A phase transition was observed around 300 °C with low permittivity values $\epsilon' \approx 120$. A saturated hysteresis loop was obtained along the major face, with a low remanent polarization ($P_r < 0.2 \mu\text{C}/\text{cm}^2$). Ferroelectricity displayed in the major face of the grown platelets may result from the non-(00l) oriented crystallites, i.e. due to contributions from *a*–*b* planes not parallel to the major faces.

Acknowledgements

One of the authors, Harvey Amorín, acknowledges the Foundation for Science and Technology (FCT, Lisbon-Portugal) for financial support through a Ph.D. grant. We thank Eng^a M. da Conceição and Tec. M. M. do Amaral for their technical support.

References

1. Paz de Araujo, C. A., Cuchiari, J. D., McMillan, L. D., Scott, M. C. and Scott, J. F., Fatigue-free ferroelectric capacitors with platinum electrodes. *Nature*, 1995, **374**, 627–629.
2. Amanuma, K., Hase, T. and Miyasaka, Y., Preparation and ferroelectric properties of $\text{SrBi}_2\text{Ta}_2\text{O}_9$ thin films. *Appl. Phys. Lett.*, 1995, **66**, 221–223.
3. Scott, J. F., Ross, F. M., Paz de Araujo, C. A., Scott, M. C. and Huffman, M., Structure and device characteristics of $\text{SrBi}_2\text{Ta}_2\text{O}_9$ -based nonvolatile random-access memories. *Mater. Res. Soc. Bull.*, 1996, **21**, 33–39.
4. Aurivillius, B., Mixed bismuth oxides with layer lattices, I., The structure type of $\text{CaNb}_2\text{Bi}_2\text{O}_9$. *Arkiv for Kemi*, 1949, **1**, 463–480.
5. Subbarao, E. C., Crystal chemistry of mixed bismuth oxides with layer-type structure. *J. Am. Chem. Soc.*, 1962, **45**, 166–169.
6. Dat, R., Lee, J. K., Auciello, O. and Kingon, A. I., Pulsed laser ablation synthesis and characterization of layered $\text{Pt}/\text{SrBi}_2\text{Ta}_2\text{O}_9/\text{Pt}$ ferroelectric capacitors with practically no polarization fatigue. *Appl. Phys. Lett.*, 1995, **67**, 572–574.
7. Al-Shareef, H. N., Dimos, D., Boyle, T. J., Warren, W. L. and Tuttle, B. A., Qualitative model for the fatigue-free behavior of $\text{SrBi}_2\text{Ta}_2\text{O}_9$. *Appl. Phys. Lett.*, 1996, **68**, 690–692.
8. Taylor, D. J., Jones, R. E., Zucher, P., Chu, P., Yui, Y. T., Jiang, B. and Gillespie, S. J., Electrical properties of $\text{SrBi}_2\text{Ta}_2\text{O}_9$ thin films and their temperature dependence for ferroelectric nonvolatile memory applications. *Appl. Phys. Lett.*, 1996, **68**, 2300–2302.
9. Boyle, T. J., Buchheit, C. D., Rodriguez, M. A., Al-Shareef, H. N., Hernandez, B. A., Scott, B. and Ziller, J. W., Formation of $\text{SrBi}_2\text{Ta}_2\text{O}_9$: Part I. Synthesis and characterization of a novel sol-gel solution for production of ferroelectric $\text{SrBi}_2\text{Ta}_2\text{O}_9$ thin films. *J. Mater. Res.*, 1996, **11**, 2274–2281.
10. Susuki, M., Nagasawa, N., Machida, A. and Ami, T., Preparation of layered ferroelectric $\text{Bi}_2\text{SrTa}_2\text{O}_9$ single-crystal platelets. *Jpn. J. Appl. Phys.*, 1996, **35**, L564–L567.
11. Machida, A., Nagasawa, N., Ami, T. and Suzuki, M., Ferroelectricity of $\text{Bi}_2\text{SrTa}_2\text{O}_9$ single crystals grown by the self-flux method. *Jpn. J. Appl. Phys.*, 1997, **36**, 7267–7271.

12. Sih, B., Tang, J., Dong, M. and Ye, Z. G., Ferroelectric $\text{SrBi}_2\text{Ta}_2\text{O}_9$ single-crystal growth and characterization. *J. Mater. Res.*, 2001, **16**, 1726–1733.
13. Elwell, D. and Sheel, H. J., *Crystal Growth from High Temperature Solution*. Academic Press, New York, 1975.
14. Tolksdorf, W., *Handbook of Crystal Growth: Flux Growth*. Elsevier Science, North Holland, 1994.
15. Machida, A., Nagasawa, N., Ami, T. and Suzuki, M., Domain motion of ferroelectricity of $\text{Bi}_2\text{SrTa}_2\text{O}_9$ single crystals under an ac-voltage electric field. *Jpn. J. Appl. Phys.*, 1999, **37**, 795–799.
16. Rae, A. D., Thompson, J. G. and Withers, R. L., Structure refinement of commensurately modulated bismuth strontium tantalate, $\text{Bi}_2\text{SrTa}_2\text{O}_9$. *Acta Cryst.*, 1992, **B48**, 418–428.
17. Shimakawa, Y., Kubo, Y., Nakagawa, Y., Kamiyama, T., Asano, H. and Izumi, F., Crystal structures and ferroelectric properties of $\text{SrBi}_2\text{Ta}_2\text{O}_9$ and $\text{Sr}_{0.8}\text{Bi}_{2.2}\text{Ta}_2\text{O}_9$. *Appl. Phys. Lett.*, 1999, **74**, 1904–1906.
18. Noguchi, Y., Direct evidence of A-site-deficient strontium bismuth tantalate and its enhanced ferroelectric properties. *Phys. Rev. B*, 2001, **63**, 214102.